MINISTRY OF EDUCATION AND TRAINING
HA NOI NATIONAL UNIVERSITY OF EDUCATION

NGUYEN THI THU TRANG

A THEORETICAL STUDY OF THE X–H···O/N (X = C, N) HYDROGEN BONDS USING QUANTUM CHEMICAL METHOD

Major: Theoretical and Physical Chemistry
Code: 62.44.01.19

SUMMARY OF CHEMICAL PhD THESIS

HA NOI - 2018

THE WORK IS COMPLETED AT
HA NOI NATIONAL UNIVERSITY OF EDUCATION

***Supervisor*: 1. Assoc. Prof. Dr. Nguyen Tien Trung**
2. Assoc. Prof. Dr. Tran Thanh Hue

Reviewer 1: Prof. Dr. Lam Ngoc Thiem
(University of Science - VNU)

Reviewer 2: Assoc. Prof. Dr. Le Kim Long
(University of Education - VNU)

Reviewer 3: Assoc. Prof. Dr. Huynh Dang Chinh
(Ha Noi University of Science and Technology)

The thesis will be defended at Boad in Ha Noi National University of Education, meeting in ….. at … o'clock, date ….., month….., year 2018

Reading the thesis at:
- The national library of Viet Nam, Ha Noi
- The information Center - library of Ha Noi national university of education

1. Introduction

Non-covalent interaction is a typical interaction that plays a key role in many fields of sciences and life aspects. For example, they determine the structure of liquids and the large biomolecules such as DNA/RNA, proteins; contribute to the solvation phenomena, the physical adsorption on surfaces as well as take a role in the life processes. Among these interactions, the X–H···Y hydrogen bond is the most typical representative because of its importance in the solution processes, the arrangement of molecules in crystals and supramolecules. Especially, the existence of thousands of the C–H···O/N and N/O–H···O/N hydrogen bonds that have been found in the crucial biomolecules is a further evidence of the importance of hydrogen bond.

Up to now, the hydrogen bond is mainly classified into two groups: the classical hydrogen bond or red-shifting hydrogen bond (RSHB) and blue-shifting hydrogen bond (BSHB). The concept of red-shifting hydrogen bond is probably introduced first by Pauling, and then the properties of hydrogen bond have been intensively investigated both theoretically and experimentally. Generally, this kind of hydrogen bond is electrostatic in nature, and its characteristics are the elongation of X–H bond along with the decrease of its corresponding stretching vibrational frequency upon the complexation. Meanwhile, the BSHB, which has been observed experimentally the first time by Sandorfy and co-workers in 1980, behaves the opposite characteristics as compared to the RSHB. In 1997, then Boldesku reported that the blue shifts of C-H/D covalent bonds belonging to haloforms as they interact with the series of proton acceptors in solution. Sequentially, the first observation of the blue shifts in gaseous phase was reported in 1999 when the interactions between CHF_3, $CHCl_3$ and C_6H_5F with each other formed. These investigations have been required the scientists to draw their attentions to the origin of the new kind of hydrogen bond. The first systematic investigation of the BSHB was carried out by Hobza and his colleagues. From this point, there have been a large number of theoretical studies using computational chemical methods conducted with aim to explain the origin of the BSHB. Even though the characteristics of the BSHB are well established, the nature of the blue shifts has been the subject of intense debate, and whether or not there are differences between two kinds of hydrogen bonds. A number of hypotheses and models have been proposed to get insight their origin, however, no general interpretation has been successfully applied to all the hydrogen bonded complexes that possess the BSHB. In general, each scheme has some advantages and limitations, and they all rationalize the phenomenon on the basis of dimer properties when the H-bonded complexes are already formed.

In 2011, Roman Szostak indicated that charge on H atom of isolated proton donor in the X–H···Y hydrogen bond might be applied to predict which type of the hydrogen bond is formed. Particularly, the blue shifts can be observed when the charge on H atoms is less positive, by contrast, the larger charge on H atom can facilitate the red-shifting hydrogen bond formation. Remarkably, a very recent study on nature of the hydrogen bond by means of valence bond self-consistent field (VBSCF) method stated that the origin of the red- or blue-shifts was resulted from the competition between covalent and ionic characteristics of X–H proton donors. These results showed that the formation of the hydrogen bond depends on the properties of the isolated proton donors.

In Viet Nam, the blue shifting hydrogen bond has started studying since 2002 and has been continuing. There are two main reseach groups in this field in Viet Nam, which are the group of Assoc.Prof.Dr Nguyen Thi Minh Hue, Ha Noi national university of education, and Assoc.Prof.Dr Nguyen Tien Trung – Quy Nhon university. The preceding research by Assoc.Prof. Dr Nguyen Tien Trung has stated that the origin of the BSHB and the RSHB is influenced by the polarity of X-H proton donor and the gas phase basicity at Y of proton acceptor. With the interesting results obtained from this research direction, it is necessary to carry out the systematic research that allow us to propose a more general rules/hypothesis for the origin of hydrogen bond on the basis of inherent properties of proton donor and proton acceptor.

As mentioned above, the X–H···O/N hydrogen bonds (X = C, N) have recently been discovered in the biological structures of life, therefore, understanding the nature of these hydrogen bonds plays a very essential role. The results from experimental and theoretical studies have shown the blue shift of the C–H···O hydrogen bonds. Notably, the blue-shifting N–H···O hydrogen bonds have recently been also detected in the complexes with HNO and HNS molecules acting as proton donor. Currently, the investigations into this kind of hydrogen bonds which are present in complexes close to the structure of proteins, DNA, RNA are of interest in research. However, the origin of the C–H···O and N–H···O blue-shifting hydrogen bonds has not clarified. Thus, carrying out continuously the systematic studies of these two types of hydrogen bonds on the basis of the isolated monomers as well as looking for molecular systems containing them with aim to understand their nature are extremely necessary. Furthermore, the comparison of magnitude of the blue shift of C–H and N–H covalent bonds involved in the hydrogen bonds X–H···O/N (X = C, N) and their stability following complexation are also crucial. It is expected to clarify the origin of the blue-shifting hydrogen bond and the classification of hydrogen bond. More importantly, it is also helpful to know further properties of the other weak interactions in DNA, RNA, protein, and to help for synthesizing drugs for life and human health.

Along with the above issues, we also consider to evaluate the stability of other non-covalent interactions such as Lewis acid-base interaction, chalcogen-chalcogen, π···π interactions,… as well as their characteristics together with the hydrogen bonds in stabilizing complexes. These interactions play a very important role in supramolecular synthesis, crystal design, separation and extraction and biology.

For all the above reasons we have arrived at the decision to choose the research topic: "***A theoretical study of the X–H···O/N (X = C, N) hydrogen bonds using quantum chemical method***".

2. Objectives

❖ Search the complexes involving the C/N–H···O blue-shifting hydrogen bonds which facilitate classification of hydrogen bond based on the isolated monomers. At the same time, this serves as a supplement that enriches the knowledge of this new bond.

❖ Make a comparison of the C–H···O and the N–H···O hydrogen bonds in terms of formation, stability and their origin. The obtained results in this work and the previous ones help to contribute to putting forward a fundamental theory for classifying the hydrogen bond.

❖ Investigate the formation and nature of some noncovalent interactions such as acid-base Lewis, chalcogen-chalcogen,… and their role together with the hydrogen bond in stabilizing the obtained complexes.

❖ Evaluate the contribution of energy components into total interaction energy of the complexes in order to understand further the nature of the formation of interactions and complexes.

3. The innovations

❖ Having provided the basic foundations of the origin and classification of hydrogen bonds with C/N–H proton donors which are particularly reliant on the polarity of the C/N–H bonds and the gas phase basiciy of proton acceptors.

❖ The stability of the N/C–H···O/N hydrogen bonds is quantitative and compared systematically and thoroughly, especially in the complexes of nucleobases. The blue shift of C–H involved in the hydrogen bonds decreases in the order of C_{sp3}–H > C_{sp2}–H >C_{sp}–H.

❖ Having found the π···π* interaction contributing to stability of the complexes between CO_2-philic compounds and CO_2 for the first time. Notably, the C–H···O blue-shifting hydrogen bond has been observed in the complexes of metanol and etanol with CO_2, which has not been reported previously.

❖ The results of the SAPT2+ analysis indicate that a dominant role of the electrostatic energy term along with an addition of the dispersion and induction energy components contributes to stabilization of hydrogen bond and complex.

4. The scientific and practical significance of the thesis

The dissertation has provided a scientific basis for understanding the nature and classification of the red- and blue-shifting hydrogen bond with the involvement of C/N–H covalent bonds acting as proton donors, which are based on the polarity of the C/N–H bonds and the gas phase basicity of the proton acceptors. This is an important basis for putting forth a more general model/hypothesis of classification of hydrogen bonds in the next future. The obtained results help to determine the influences of different weak interactions on living structures such as DNA, RNA and proteins. Moreover, the clarification of the strength and nature of hydrogen bonded interactions, especially hydrogen bonds with the involvement of C–H bond, also help to orient for developing new drugs and materials for life and human health. Notably, the results are useful documents for students, graduate students and tearchers in scientific research and teaching. They are valuable references for relevant studies on weak interactions, particularly hydrogen bonds.

Understanding the formation, durability of noncovalent interactions such as the Lewis acid-base, chalcogen-chalcogen,…and the first detection of the contribution of π···π* interaction to stabilization of complexes involved CO_2 and presence of the C–H···O blue-shifting hydrogen bonds in the complexes of methanol and ethanol with CO_2 are found, which have not previously published, which helps to use effectively the supercritical CO_2 solvents in the separation, extraction, synthesis of valuable compounds, and search for materials to adsorb the gas phase CO_2.

Chapter 1. THE FUNDAMENTAL THEORY OF QUANTUM CHEMISTRY

Introducing the Schrödinger equation, multiple-particle wave functions, basis set; brief introduction of Basis Set Superposition Error (BSSE); introduction of the basis

of quantum chemical approximation methods; introduction to AIM, NBO theory, and SAPT methods.

Chapter 2. OVERVIEW OF WEAK INTERACTIONS, HYDROGEN BOND AND RESEARCH SYTEMS

Overview of some weak interactions; Introduction of the importance, concepts, classifications, and computational methods of the hydrogen bond; Overview of the research system. The dissertation focuses on the following interaction systems:

- Interactions between C_2H_4, C_2H_3X, XCH=CHX (X = F, Cl, Br) and CO_2
- Interactions between XCH_2OH (X = H, CH_3, F, Cl, Br) and CO_2
- Interactions between CH_3SZCHX_2 (X = H, CH_3, F, Cl, Br; Z = O, S) and CO_2
- Interactions between CH_3COCHR_2 (R = H, CH_3, F, Cl, Br) and CO_2 và XCN (X = F, Cl, Br)
- Interactions between NH_2CHO, XNHCHO (X = F, Cl, Br, CH_3) and H_2O
- Interactions between RCHO and CH_3CHO (R = H, CH_3, F, Cl, Br)
- Interactions between RCHO and XCN (R = H, F, Cl, Br, CH_3, NH_2; X= H, F)
- Interactions between cytosine and guanine

Computational methods

The optimized geometries for all structures of monomers and complexes were carried out using the Moller-Plesset perturbation theory (MP2), the density functional theory (B3LYP) with high correlation consistent basis sets, including 6-311++G(2d,2p), 6-311++G(3df,2pd), aug-cc-pVDZ and aug-cc-pVTZ. Selected levels of theory are good in geometric guess, interaction energy for the weak interaction complexes, hydrogen bonds. The stretching vibrational frequencies were calculated to ensure that the optimized geometries were all minima energy on potential energy surfaces, and to estimate zero-point energy (ZPE). To avoid vibrational couplings between the CH_3 stretching modes of CH_3SZCH_3, $CH_3SZCH(CH_3)_2$ (Z = O, S) and the NH_2 stretching modes of NH_2CHO, guanine, cytosine, the harmonic frequencies in these monomers and relevant complexes were calculated by means of the deuterium isotope effect. Single point energies for all monomers and complexes examined were calculated using coupled-cluster theory CCSD(T) with the high basis sets (aug-cc-pVTZ, 6-311++G(3df,2pd) based on the optimized geometries. Basis set superposition errors (BSSE) which were calculated by using the counterpoise method of Boys and Bernadi were evaluated with the same level of theory as energy calculations. Interaction energy of each complex is thus derived as the difference in the total energy of the complex and the sum of relevant monomers, corrected for ZPE only ($\Delta E = E_{complexes} - (E_{monomer1} + E_{monomer2})$) or for both ZPE and BSSE ($\Delta E^* = \Delta E + BSSE$). Deprotonation enthalpy (DPE) is the enthalpy change in the reaction in the gas phase: $AH \rightarrow A^- + H^+$, and the proton affinity (PA) is the negative of the enthalpy change in the reaction in the gas phase: $A + H^+ \rightarrow AH^+$. All electron structure calculations were performed using Gaussian 03 (E.01) or Gaussian 09 (A.02) software. Topological geometry, electron density ($\rho(r)$), Laplacian of electron density ($\nabla^2(\rho(r))$) at bond critical points (BCPs) were calculated based on the AIM theory using AIM 2000 software. Electron potential energy density (V(r)) and electron kinetic energy density (G(r)) at BCPs are calculated as follow: $G(r) = \frac{3}{10}(3\pi^2)^{2/3}\rho^{5/3}(r) + \frac{1}{6}\nabla^2\rho(r)$; $V(r) = \frac{1}{4}\nabla^2\rho(r) - 2G(r)$. The electron properties of monomers and complexes were evaluated by NBO analysis using the NBO software 5.G. In order to evaluate the contribution of energy components to total

stabilization energy, the symmetry-adapted perturbation theory (SAPT2+) approach with the selected basis sets is applied, which is calculated by the Psi4 package. The total interaction energy by the SAPT2+ approach can be decomposed into the four fundamental components: electrostatic (as Coulomb attraction, E_{elest}), induction (E_{ind}), dispersion (E_{disp}) and exchange (or Pauli repulsion, E_{exch}). Accordingly, the total interaction energy derived by means of SAPT can be calculated as follows: $E^{SAPT2+} = E_{elest} + E_{ind} + E_{disp} + E_{exch} + \delta E^{HF}$, where δE^{HF} includes the third and higher-order induction and exchange-induction terms. Furthermore, some other sofwares, such as Gaussview, Molden, Corel Draw, Origin, … were also used.

Chapter 3. RESULTS AND DISCUSSION

3.1. Interaction of ethylene, its double halogenated derivatives (XCH=CHX) with CO_2

3.1.1. *Interaction of ethylene with CO_2*

The shapes of the six stable complexes, which belong to C_{2v} point group, between ethylene and carbon dioxide and their AIM analysis at the MP2/aug-cc-pVDZ level are shown in Fig. 3.1(denoted hereafter by **P1**, **P2**, **P3**, **P4**, **P5** and **P6**). Their interaction energies corrected by ZPE (ΔE) and both ZPE +BSSE (ΔE^*) at the CCSD(T)/aug-cc-pVTZ//MP2/aug-cc-pVDZ level, typical results of topological analysis and distance changes of the C–H covalent bond involved in hydrogen bond at the MP2/aug-ccpVDZ are collected in Table 3.1.

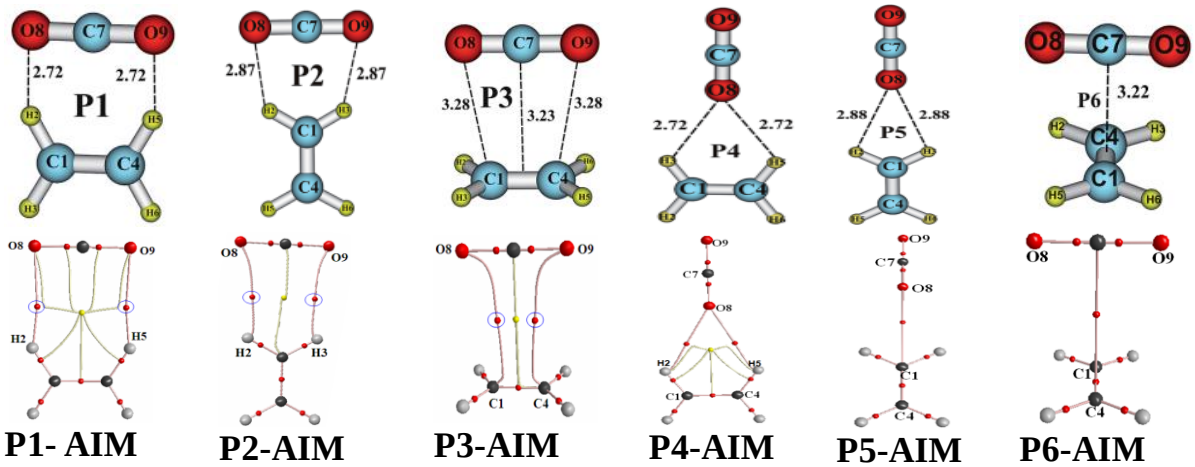

Figure 3.1. The shapes and topological geometrics of complexes formed between CO_2 and ethylene (distances given in Å)

Table 3.1. Some of parameters for the obtained complexes

Complexes	**P1**	**P2**	**P3**	**P4**	**P5**	**P6**
ΔE^*/kJ.mol^{-1}	-2.4	-1.5	-4.5	-1.5	-1.1	-4.9
$\nabla^2(\rho(O\cdots H)/(O\cdots C))$/au	0.0202	0.0181	0.0205	0.0216	0.0202	0.0226
H(r)/au	0.0007	0.0009	-	0.0009	0.0012	-
Δr(C–H)/mÅ	-0.1	0.2	-	-0.5	-0.5	-
Δν(C–H)/cm^{-1}	1.0	-4.7	-	4.0	5.6	-

Figure 3.1 and Table 3.1 indicate the presence of two C–H···O hydrogen bonds in the complexes of **P1**, **P2**, **P4** and **P5**, and all of them are weak hydrogen bonds due to both positive values of $\nabla^2(\rho(r))$ and H(r) at BCPs of these contacts. Two C–H···O hydrogen bonds in **P1**, **P4** and **P5** are blue-shifting hydrogen bonds, while they are red-shifting hydrogen bonds in **P2** (*cf.* Table 3.1). NBO results show that there is an electron density

transfer from the lone pairs n(O) and π(C=O) orbital of CO_2 to the π*(C1=C4) orbital of C_2H_4 (*ca.* 2.3 and 1.5 kJ.mol^{-1}, respectively) in **P3**. Otherwise, the electron density is transferred from the π(C1=C4) (C_2H_4) to π*(C=O) (CO_2) orbital with a value of 3.6 kJ.mol^{-1}. These results indicate the existence of π···π* and p···π* interactions in **P3**. For the complex **P6**, the π···π* intermolecular interaction from the π(C=C) to π*(C=O) orbital plays a main role in stabilizing the complex (value of hyperconjugative interaction energy to be *ca.* 4.6 kJ.mol^{-1}). The contribution of π···π* interaction to the strength of complexes between CO_2 and CO_2-philic compounds has not been reported yet in the literature.

The interaction energies of complexes range from -1.1 to -4.9 kJ.mol^{-1} with both ZPE and BSSE corrections, and decrease in the order **P6** > **P3** > **P1** > **P4** > **P2** > **P5**. It is remarkable that **P6** has not been reported yet in literature. The most stable structure of C_2H_4···CO_2 is in a good agreement with the prediction reported by Miller et al. that CO_2 lies above the plane of C_2H_4, with CO_2 axis parallel to this plane, but not parallel to C=C axis of C_2H_4.

3.1.2. Interactions of XCH=CHX (X = F, Cl, Br) with CO_2

Six stable shapes of the complexes between XCH=CHX···CO_2 with X = F, Cl and Br, optimized at the MP2/aug-cc-pVDZ level, are presented in Fig. 3.4. The complexes are denoted by **C1X**, **C2X** and **C3X** for *cis*-XCH=CHX···CO_2 complexes, and **T1X**, **T2X** and **T3X** for *trans*-XCH=CHX···CO_2 complexes (X = F, Cl and Br). Interaction energies, computed at the CCSD(T)/aug-cc-pVTZ//MP2/aug-cc-pVDZ level, and some selected geometric parameters are gathered in Table 3.6.

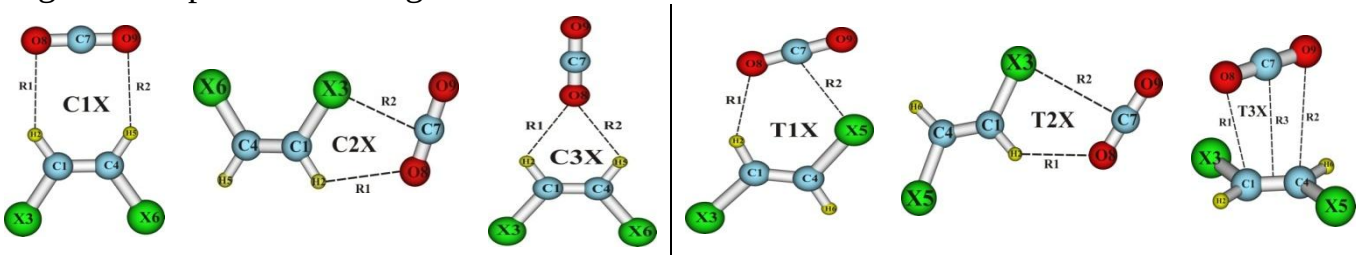

a) *cis*-XCH=CHX···CO_2 complexes | **b) *trans*-XCH=CHX···CO_2 complexes**

Figure 3.4. The shapes of XCH=CHX···CO_2 complexes (X = F, Cl and Br)

Figure 3.4 and Table 3.6 point out that the formation of the complexes **C1X** and **C3X** is thus due to the C-H···O hydrogen bonds, whereas the stability of the complexes **C2X**, **T1X** and **T2X** is contributed by both the C-H···O hydrogen bond and C-X···C Lewis acid-base interaction. In **T3X**, this is due to a p···π* interaction from n(O) to π*(C=C) orbital and a π···π* interaction from MO-π(C=O) to MO-π*(C=C). In summary, substitution of two H atoms in ethylene by two halogen X atoms induces an formation of C-X···C Lewis acid-base interaction, C-H···O hydrogen bond, π···π* and p···π* interaction contributing further to the stability of the complexes.

In general, the interaction capacity of the complexes are stronger for the *cis*-XCH=CHX···CO_2 than for the *trans*-XCH=CHX···CO_2 and both of them are more stable than the parent CH_2=CH_2···CO_2. The interaction energies corrected by ZPE and BSSE are in the range from -1.7 to -7.5 kJ.mol^{-1}, and between -4.4 and -6.8 kJ.mol^{-1} for *cis*-XCH=CHX···CO_2 and *trans*-XCH=CHX···CO_2, respectively (*cf.* Table 3.6). Hence substitution of the two H atoms in CH_2=CH_2 by two X halogens actually increases the strength of interaction of XCH=CHX with CO_2.

For both *cis*-XCH=CHX···CO_2 and *trans*-XCH=CHX···CO_2, with the same geometrical structure of each complex shape, the stability of complexes increases in the ordering of substituted derivatives going from F to Cl and then to Br (cf. Table 3.6). As the results in Table 3.8, the DPE of the C–H bond involved in the hydrogen bond decreases in the order of F > Cl > Br, whereas the PA at the X site increases in going from F via Cl to Br, in both *cis*-XCH=CHX and *trans*-XCH=CHX. Thus, the contribution of C–H···O hydrogen bond and C–X···C Lewis acid-base interaction to the stability of *cis*- and *trans*-XCH=CHX···CO_2 complexes is enhanced in the order of F to Cl and then to Br. This renders the strength of complexes increasing in the similar trend, which is consistent with the values of interaction energy given in Table 3.6. The complexes **C2X**, **T1X** and **T2X** are more stable than the remaining ones. This emphasizes a larger role of the C–X···C Lewis acid-base interaction as compared to the C–H···O hydrogen bond in stabilizing the complexes. Accordingly, substitution of two H atoms in CH_2=CH_2 by the same halogen atoms decreases the role of the π···π* interaction in stabilizing the parent C_2H_4···CO_2 complex as compared to the XCH=CHX···CO_2 complex.

Table 3.6. Interaction energies (in kJ.mol^{-1}), intermolecular contact distances (in Å), ∠OCO angle of CO_2 (^{o}) and changes of the bond length C=O (in Å)

Complexes	ΔE	ΔE*	R1	R2(R3)	$\angle O_9C_7O_8$	$\Delta r(C_7O_8)$	$\Delta r(C_7O_9)$
C1F	-3.7	-1.7	2.67	2.67	179	0.0002	0.0002
C1Cl	-4.3	-1.8	2.63	2.63	179	0.0002	0.0002
C1Br	-5.9	-2.2	2.61	2.61	179	0.0002	0.0002
C2F	-8.5	-6.6	2.59	2.88	179	0.0015	-0.0021
C2Cl	-9.4	-7.2	2.49	3.30	179	0.0014	-0.0018
C2Br	-11.3	-7.5	2.48	3.42	179	0.0015	-0.0017
C3F	-6.4	-4.4	2.65	2.65	180	0.0014	-0.0018
C3Cl	-7.0	-4.5	2.59	2.59	180	0.0015	-0.0019
C3Br	-8.1	-4.8	2.58	2.58	180	0.0015	-0.0019
T1F	-8.7	-6.5	2.50	2.90	179	0.0012	-0.0020
T1Cl	-9.0	-6.6	2.40	3.33	179	0.0011	-0.0016
T1Br	-11.1	-6.8	2.39	3.43	179	0.0011	-0.0016
T2F	-8.1	-6.3	2.60	2.88	179	0.0012	-0.0018
T2Cl	-8.8	-6.6	2.50	3.31	179	0.0013	-0.0016
T2Br	-10.6	-6.8	2.48	3.42	179	0.0013	-0.0016
T3F	-7.0	-4.4	3.25	3.25(2.80)	180	-0.0001	-0.0001
T3Cl	-9.6	-6.3	3.18	3.18(2.73)	180	-0.0001	-0.0001
T3Br	-12.8	-6.7	3.16	3.16(2.71)	180	-0.0001	-0.0001

Table 3.8. PA at the X atoms and DPE(C–H) (kJ.mol^{-1}) of the C–H bonds in XCH=CHX (X = H, F, Cl, Br)

	CH_2=CH_2	*cis*-XCH=CHX			*trans*-XCH=CHX		
X	H	F	Cl	Br	F	Cl	Br
PA		547	624	656	541	611	640
DPE	1717	1626	1577	1556	1620	1581	1565

As pointed out from Table 3.9, there is a small contraction of C–H bond length (*ca.* 0.2-1.2 mÅ) and an increase of its stretching frequency (*ca.* 0.7-12.6 cm^{-1}) in the

complexes examined, except for **C1F** with a C–H slight bond length elongation of 0.1 mÅ and a corresponding stretching frequency decrease of 1.7 cm^{-1}. Accordingly, the C–H···O hydrogen bond belongs to the blue-shifting hydrogen bond in all complexes, except for **C1F** being a red-shifting hydrogen bond. Substitution of two H atoms in C_2H_4 by two alike halogen atoms tends to induce a larger blue shift of the C–H bond in the C–H···O hydrogen bond in both *cis*- and *trans*-XCH=CHX···CO_2 complexes as compared to the parent CH_2=CH_2···CO_2, even though the polarity of the C–H bond is weaker in CH_2=CH_2. This result suggests that the magnitude of C–H bond length contraction and its stretching frequency increase upon complexation depend on the geometric shape of the complex formed and the polarity of C–H bond involved in hydrogen bond in the isolated monomers.

Table 3.9. Change of C–H bond length (Δr, in mÅ) and its corresponding stretching frequency (Δν, in cm^{-1}) in the complexes

Complexes	**C1F**	**C1Cl**	**C1Br**	**C2F**	**C2Cl**	**C2Br**
Δr(C1−H2)	0.1(0.1)	-0.2(-0.2)	-0.4(-0.4)	-1.0	-0.5	-0.4
Δν(C1−H2)	-1.7(-1.7)	0.7(0.7)	1.5(1.5)	7.1	4.5	3.3
Complexes	**C3F**	**C3Cl**	**C3Br**	**T1F**	**T1Cl**	**T1Br**
Δr(C1−H2)	-1.2(-1.2)	-1.2(-1.2)	-1.2(-1.2)	-0.8	-0.9	-0.9
Δν(C1−H2)	12.6(12.6)	10.8(10.8)	10.9(10.9)	8.6	9.6	10.6
Complexes	**T2F**	**T2Cl**	**T2Br**	-	-	-
Δr(C1−H2)	-0.8	-0.3	-0.3	-	-	-
Δν(C1−H2)	8.0	5.6	5.4	-	-	-

The values in the blanket are for C4–H5 bond

The selected NBO results are given in Table 3.10. The presence of the C–H···O hydrogen bond and C–X···C Lewis acid-base interaction in the complexes **C2X**, **T1X** and **T2X** is firmly indicated by means of EDT from n(O) to σ*(C1–H2) orbital with hyperconjugative energies of 3.0-11.3 $kJ.mol^{-1}$ and from n(X) to π*(C=O) orbital with hyperconjugative energies of 3.3-4.2 $kJ.mol^{-1}$. For **C1X** and **C3X**, their complexation is only due to the C–H···O hydrogen bond, which is supported by the values of hyperconjugation energy of 0.9-4.0 kJ mol^{-1} in EDT from n(O) to σ*(C–H) orbital.

A positive EDT value implies an electron density transfer from XCH=CHX to CO_2 in **C1X**, **C3X**, **T1X**, **T2X** and **T3X**, while reversed transfers are observed for **C2X**. This implies that a larger role of the C-H···O hydrogen bond relative to the C–X···C Lewis acid-base interaction contributes to the total stabilization energy of the complexes including **C1X**, **C3X**, **T1X**, **T2X** and **T3X**. On the other hand, the stability of **C2X** is mainly determined by C–X···C Lewis acid-base interaction overcoming the C–H···O hydrogen bond.

The existence of weak interaction p···π* in **T3X** is identified due to the EDT from n(O) orbital of CO_2 to π*(C=C) orbital of *trans*-XCH=CHX, with hyperconjugative energy of 1.5-2.1 $kJ.mol^{-1}$. In addition, as a result of complexation, electrons are transferred from π(C=C) to π*(C=O) and from π(C=O) to π*(C=C). The corresponding hyperconjugative energies are indeed in the range of 3.5-5.1 $kJ.mol^{-1}$ for the former and 1.1-2.6 $kJ.mol^{-1}$ for the latter. This indicates the presence of π···π* weak interaction in stabilizing **T3X**. Consequently, the stability of **T3X** is contributed

by the weak interactions p···π* and π···π*. Table 3.10 show that, the increase of C1(C4) s-character, overcoming the enhancement in the population of the σ*(C1–H2) and σ*(C4–H5) orbitals, plays a decisive role in giving rise to a length contraction and a stretching frequency increase of the C1–H2 and C4–H5 bonds. Nevertheless, the red shift of C1–H2 and C4–H5 stretching frequencies in **C1F** are determined by the increase of 0.0013 electron in the population of the σ*(C1–H2) and σ*(C4–H5) orbitals overcoming the slight increase of 0.26% in the C1(H2) and C4(H5) scharacter percentage upon complexation.

Table 3.10. NBO analysis of the XCH=CHX···CO_2 complexes (X = F, Cl, Br)

Complexes	EDT (e)	Δσ*(C-H) (e)	Δ%s(C) (%)	E_{inter}(n(O)) → σ*(C–H)) (kJ.mol^{-})[1]	E_{inter}(n(X) →π*(C=O) (kJ.mol^{-1})	ΔE_{intra}(n(X) → σ*(C–H) (kJ.mol^{-1})
C1F	-0.0061	0.0013	0.26	3.43[a] 0.88[b]	-	-1.17
C1Cl	-0.0076	0.0015	0.29	3.85[a] 0.96[b]	-	-1.59
C1Br	-0.0082	0.0015	0.33	3.97[a] 0.92[b]	-	-1.51
C2F	0.0001	0.0002	0.47	3.10	4.06	-2.76
C2Cl	0.0002	0.0011	0.54	5.77	3.93	-1.92
C2Br	0.0003	0.0013	0.50	6.07	4.20	-1.46
C3F	-0.0029	0.0004	0.27	2.68	-	-1.34
C3Cl	-0.0039	0.0005	0.30	3.18	-	-1.26
C3Br	-0.0041	0.0006	0.32	3.14	-	-0.92
T1F	-0.0016	0.0012	0.44	6.61	3.18	-0.92
T1Cl	-0.0032	0.0021	0.61	10.75	3.31	-1.34
T1Br	-0.0031	0.0022	0.66	11.30	3.51	-1.05
T2F	-0.0003	0.0004	0.44	3.39	4.02	-1.80
T2Cl	-0.0001	0.0014	0.54	5.98	3.89	-1.09
T2Br	-0.0002	0.0015	0.56	6.32	4.14	-0.71
T3F	-0.0003	-	-	1.51[c]	1.09[d]	3.52[e]
T3Cl	-0.0009	-	-	2.13[c]	1.76[d]	4.77[e]
T3Br	-0.0007	-	-	1.84[c]	2.59[d]	5.06[e]

[a]C4-H5 bond, [b]C1–H2 bond, [c]from n(O) to π(C=C) orbital, [d]from π(C=O) to π*(C=C) orbital, [e]from π(C=C) to π*(C=O) orbital*

Summary

- The stabilization of the parent complex C_2H_4···CO_2 is determined by the π···π* interaction. The strength of the halogenated derivatives is stabilized by hydrogen bonds, Lewis acid–base interaction, p···π* and π···π* interactions. Remarkably, the contribution of the π···π* interaction to the formation of the complexes between CO_2-philic compounds and CO_2 has been revealed for the first time.

- The substitution of H atom in C–H bond of C_2H_4 by the same halogen atom (F, Cl, Br) actually increases the strength of complexes as compared to the parent C_2H_4···CO_2 complex. The stability of complexes increases in the ordering of substituted derivatives going from F to Cl and then to Br.

- The C–H···O blue-shifting hydrogen bonds are revealed. The results show that the magnitude of C–H bond length contraction and its stretching frequency increase upon complexation is inversely proportional to the polarization of the C–H bond in the isolated monomers.

- The NBO results suggest that Lewis acid-base interaction is resulted from an electron density transfer from n(X) to π*(C=O) orbital. The transfer of electron density from n(O) to π*(C=O) orbital and from π(C=C) to π(C=O) orbital and versa are responsible for the formation of p···π* and π···π* interaction.

3.3. Interaction of the >S=O and >S=S groups in some doubly methylated and halogenated derivatives of CH_3SOCH_3 and CH_3SSCH_3 with CO_2

3.3.1. Interactions of CO_2 with CH_3SZCH_3 (Z=O, S)

Three stable shapes of the optimized structures of complexes CH_3SZCH_3···CO_2 (Z=O, S) at MP2/6-311++G(2d,2p) are presented in Figure 3.3, which are denoted hereafter by **T1**, T2 and **T3**.

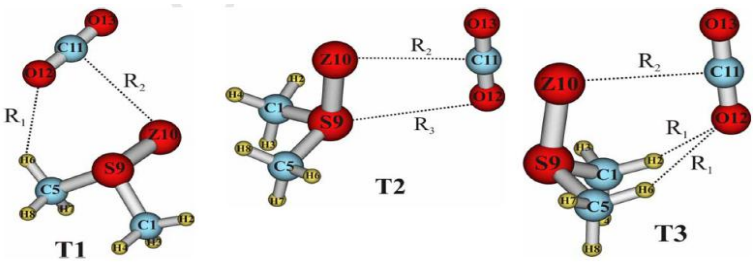

Figure 3.8. The stable shapes of complexes between CH_3SZCH_3 (Z=O, S) and CO_2

Table 3.14. Interaction energies (in kJ.mol^{-1}), contact distances (in Å), electron density and Laplacian (in au) of CH_3SZCH_3···CO_2 complexes.

	Z=O			Z=S		
	T1	**T2**	**T3**	**T1**	**T2**	**T3**
ΔE^a	-17.2	-14.3	-17.4	-17.1	-13.8	-16.9
ΔE^{*a}	-14.4	-10.9	-13.7	-14.2	-9.8	-13.2
R1 or R3	2.63	3.49	2.65	2.59	3.37	2.54
R2	2.77	2.69	2.70	3.33	3.30	3.30
$\nabla^2(\rho(Z\cdots C)/(\rho(O\cdots S))$	0.0468	0.0556	0.0536	0.0272	0.0296	0.0291
$\nabla^2(\rho(O\cdots H))$	0.0228	0.0359	0.0209	0.0258	0.0224	0.0248

[a]*Taken from MP2/aug-cc-pVTZ//MP2/6-311++G(2d,2p)*

As be seen in Figure 3.8 and Table 3.14, the Lewis acid-base, chalcogen-chalcogen and hydrogen bonded interactions are formed in the complexes, in which the strength of the **T1** and **T3** shapes is contributed by both the S=Z···C Lewis acid-base and the C–H···O hydrogen bonded interactions, while the contribution to the strength of **T2** shape arises from the S=Z···C Lewis acid-base and O···S=Z chalcogen-chalcogen interactions. The formed complexes are significantly stable with interaction energies from -9.6 to -14.5 kJ.mol^{-1} corrected by ZPE and BSSE at CCSD(T)/6-311++G(3df,2pd)//MP2/6-311++G(2d,2p) level. The strength of the CH_3SZCH_3···CO_2 (Z=O, S) complexes decreases in the order of **T1** ≈ **T3** > **T2**, in which the CH_3SOCH_3···CO_2 complexes are more stable than the corresponding CH_3SSCH_3···CO_2 ones. This is due to a larger contribution of attractive electrostatic interaction to the overall interaction energy in the complexes of CH_3SOCH_3···CO_2 compared to CH_3SSCH_3···CO_2. Remarkably, it should

be emphasized that two stable **T2** and **T3** structures of $CH_3SOCH_3\cdots CO_2$, and three stable shapes of $CH_3SSCH_3\cdots CO_2$ are revealed for the first time.

3.3.2. Interactions of CO_2 with CH_3SZCHX_2 (X=H, CH3, F, Cl, Br; Z=O, S)

We replaced two H atoms in a CH_3 group of CH_3SZCH_3 in the most stable **T1** shape of $CH_3SZCH_3\cdots CO_2$ complexes by two CH_3, F, Cl and Br alike groups to evaluate the effects of them in stabilizing the complexes as well as the type of the C–H···O hydrogen bond formed, The stable shapes of the obtained complexes are presented in Figure 3.9.

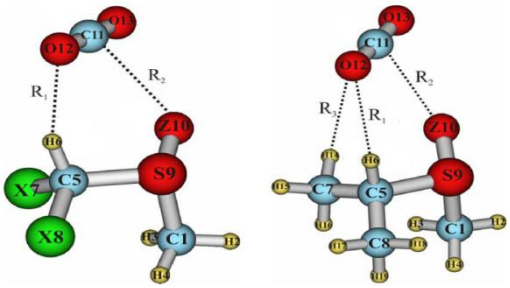

Figure 3.9. The stable shapes for interactions of $CH_3SZCH(CH_3)_2$ and CH_3SZCHX_2 (X=H, F, Cl, Br; Z=O, S) with CO_2 at MP2/6-311++G(2d,2p).

Table 3.15. Interaction energies using MP2/aug-cc-pVTZ//MP2/6-311++G(2d,2p), and proton affinities (PA) at the O and S sites and deprotonation enthalpies (DPE) of the C–H bonds involved in hydrogen bond for the isolated monomers using CCSD(T)/6-311++G(3df,2pd)//MP2/6-311++G(2d,2p) (all in kJ.mol^{-1}).

	Z = O					**Z = S**				
	H	CH_3	F	Cl	Br	H	CH_3	F	Cl	Br
ΔE^*	-14.4	-16.4	-14.7	-15.0	-16.3	-14.2	-15.5	-13.7	-14.3	-15.4
PA	900.1	904.8	876.2	876.7	884.9	907.1	911.0	883.8	891.0	896.0
DPE	1610.1	1711.9	1619.5	1560.8	1540.6	1578.4	1704.7	1606.0	1540.4	1522.0

The interaction energies are significantly negative, implying that the obtained complexes are quite stable on the potential energy surface. For the $CH_3SOCHX_2\cdots CO_2$ complexes, their strength is enhanced in the order H < F < Cl < Br < CH_3 (*cf.* Table 3.15). Accordingly, the substitution of two H atoms in a CH_3 group of CH_3SOCH_3 by two X alike groups makes the formed complexes more stable as compared to $CH_3SOCH_3\cdots CO_2$. The replacement also leads to a slight enhancement of stability of the $CH_3SSCHX_2\cdots CO_2$ complexes in the sequence from F to H to Cl to Br and to CH_3.

The gas phase basicity at the O and S sites increases in going from F to Cl to Br to H and to CH_3, and the polarity of the C-H bonds decreases in the sequence from Br to Cl to H to F and to CH_3. Accordingly, the overall stabilization energy for the $CH_3SZCH_3\cdots CO_2$ complexes is contributed by a main role of the >S=Z···C interaction and an additional cooperation of the C–H···O hydrogen bond, in which an enhanced contribution of the hydrogen bond should be suggested for the complexes from H to F to Cl and then to Br derivative.

The C–H···O hydrogen bond in all the examined complexes belongs to the blue shifting hydrogen bond (*cf.* Table 3.16). An increase in the magnitude of the C–H bond length contraction and its stretching frequency increase in the C–H···O hydrogen bonds for both $CH_3SOCH_3\cdots CO_2$ and $CH_3SSCH_3\cdots CO_2$ in the order of X

from Br via Cl and to F is observed. This trend is consistent with a decrease of the C–H polarization in the CH_3SZCHX_2 monomers. In other words, the blue shift magnitude of C–H bonds involved hydrogen bond are inversely proportional to the polarization of the C–H bond in the initial monomers. Nevertheless, there is a different tendency in the changes of the C–H bond length and its stretching frequency for $CH_3SZCH_3\cdots CO_2$, with X=H, CH_3, and Z=O, S (*cf.* Table 3.15 and Table 3.16). Therefore, it should be mentioned that the origin of blue-shifting hydrogen bond is slightly affected by the complex shape and the neighbouring intermolecular interactions, besides the crucial dependence on the polarity of covalent bond acting as the isolated proton donor.

Table 3.16. The variation of the C5–H6 bond length (Δr, mÅ), its stretching frequencies (Δm, cm^{-1}) at MP2/6-311++G(2d,2p).

	Z = O					**Z = S**				
	H	CH_3	F		Br	H	CH_3	F	Cl	Br
Δr	-0.5	-1.2(-0.2)	-2.0	-1.1	-1.0	-0.5	-1.2 (-0.4)	-1.6	-1.3	-1.0
Δν	8.3	17.6 (1.6)	27.8	19.2	17.5	9.1	17.4 (1.8)	24.6	22.6	18.7

The values given in brackets for the C7–H14 covalent bond.

Table 3.17. NBO analyses of the $CH_3SZCHX_2\cdots CO_2$ complexes at MP2/6-311++G(2d,2p)

	X	EDT (e)	Δσ*(C5-H6) $.10^3$ (e)	Δ%s (C5) (e)	E(n(O12)→ σ*(C5-H6)) ($kJ.mol^{-1}$)	E(n(Z10)→ σ*(C11=O13)) ($kJ.mol^{-1}$)
Z=O	H	5.3	0.2	0.4	1.34	14.1
	CH_3	4.1	0.3 0.3[a]	0.4 0.2[a]	0.46 0.11[a]	3.31
	F	3.1	-1.3	0.6	2.64	11.7
	Cl	3.2	-1.4	0.6	3.10	11.6
	Br	3.0	-1.1	0.7	3.14	11.8
Z=S	H	5.1	0.7	0.4	2.51	6.7
	CH_3	3.2	0.2 0.2[a]	0.4 0.3[a]	0.62 0.21[a]	1.37
	F	2.0	-0.8	0.5	5.19	6.15
	Cl	1.6	-1.3	0.7	6.61	5.52
	Br	1.3	-1.0	0.9	7.91	6.4

[a] *For C7–H14 covalent bond.*

As is shown by the Table 3.17, the electron density transfer from the n(Z) lone pairs to the π*(C=O) orbital is stronger than that from the n(O) lone pairs to σ*(C–H) orbital, affirming that the strength of the $CH_3SZCHX_2\cdots CO_2$ complexes is contributed by a key role of Lewis acid-base interaction and an additional cooperation of the hydrogen bond. Table 3.17 show that the contraction of the C–H bond and its stretching frequency increase for $CH_3SZCHX_2\cdots CO_2$ (X=F, Cl, Br) arise from both a decrease of the σ*(C–H) electron density and an increase in the s-character percentage of the C hybrid orbital, while the C–H bond length contraction and its stretching frequency blue shift for $CH_3SZCHX_2\cdots CO_2$ (X=H, CH_3) are determined by an increase in the s-character percentage of the C hybrid orbital overcoming an increase in the occupation of the σ*(C–H) orbitals.

Summary

- The stability of the complexes is contributed by the >S=O···C Lewis acid-base interaction, chalcogen-chalcogen interaction and the C–H···O hydrogen bonds. The substitution of two H atoms in a CH_3 group of CH_3SZCH_3 by two halogen and methyl groups leads to an increase in the stability of complexes in going from F via Cl, Br and finally to CH_3 derivative.

- The bond length contraction and the stretching frequency increase of C–H bonds in the C–H···O hydrogen bonds are inversely proportional to the polarization of the C–H bond in the initial monomers, and slightly dependent on the geometric structures of the complexes.

3.4. Remarkable effects of substitution on origin of the C–H···O/N hydrogen bonds formed between CH_3COCHR_2 (R = CH_3, H, F, Cl, Br) and CO_2, XCN (X = F, Cl, Br)

3.4.1. Interactions of CO_2 with CH_3COCHR_2 (R = CH_3, H, F, Cl, Br)

Four stable shapes of the complexes between CH_3COCH_3 with CO_2, which are denoted as **H1**, **H2**, **H3** and **H4**, are shown in fig 3.10. Evidence for the existence of intermolecular contacts in the complexes by means of AIM analysis is also given in fig 3.10.

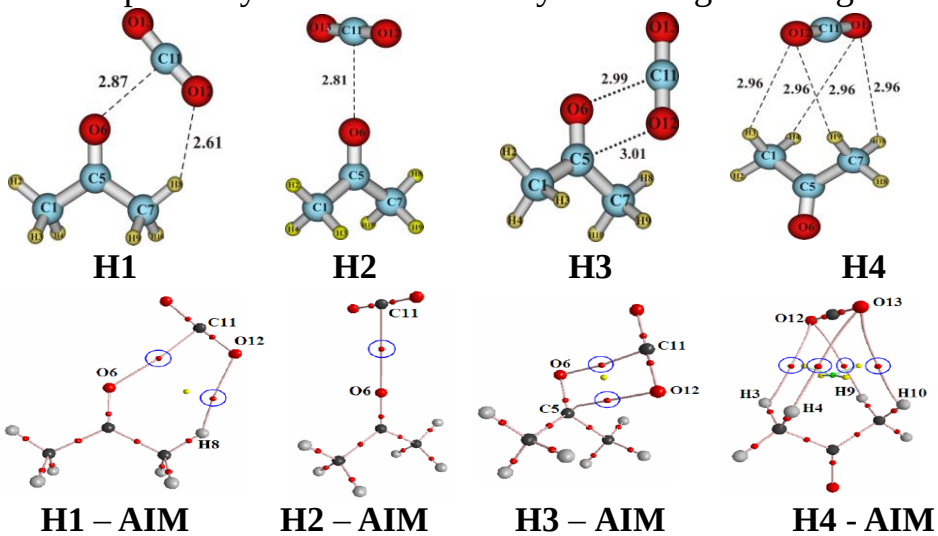

Figure 3.10. The stable shapes and topological geometries of the complexes formed between CH_3COCH_3 and CO_2

Figure 3.10 show that the Lewis acid-base interaction and hydrogen bond are formed, and both of them contribute to the strength of the complexes examined. The obtained complexes are quiet stable with the interaction energies corrected by both ZPE and BSSE for **H1**, **H2**, **H3** and **H4** to be -10.4 kJ.mol^{-1}, -9.4 kJ.mol^{-1}, -9.2 kJ.mol^{-1} and -2.4 kJ.mol^{-1}, respectively. We replaced two H atoms in a CH_3 group of CH_3COCH_3 in the most stable **H1** structure by two CH_3, F, Cl and Br alike groups (denoted by CH_3COCHR_2) in order to evaluate the stability of complexes, the origin of the C–H···O hydrogen bond formed. The stable geometries of the complexes are presented in Figure 3.11. The selected parameters of the complexes are collected in Table 3.19. The PA (using CCSD(T)/aug-cc-pVTZ//MP2/aug-cc-pVTZ) at the O site of the >C=O group and the DPE (using CCSD(T)/aug-cc-pVTZ//MP2/6-311++G(2d,2p)) of the C–H bond (–CHR_2) in isolated CH_3COCHR_2 monomers are listed in Table 3.20.

In general, the complexes are contributed by the >C=O···C Lewis acid-base interaction and the C–H···O hydrogen bond. The interaction energies are calculated to be from -11.9

to -13.8 kJ.mol^{-1} (with ZPE correction) and from -9.2 to -10.7 kJ.mol^{-1} (with ZPE + BSSE corrections) (*cf.* Table 3.19). The association of CH_3COCHR_2 with CO_2 leads to a slight increase in the interaction energy (by including both ZPE and BSSE corrections) in the order CH_3 < H ≈ Br < Cl < F. The polarization of the C–H bond increases in the order CH_3 < H < F < Cl < Br, and the gas phase basicity at the O site increases in the order F < Cl < Br < H < CH_3 (*cf.* Table 3.20). The total stabilization energy of the complexes is contributed by both the >C=O···C Lewis acid–base interaction and the C–H···O hydrogen bond, in which the crucial role of the former is suggested.

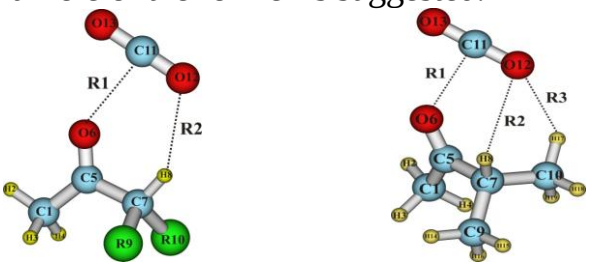

CH_3COCHR_2···CO_2 $CH_3COCH(CH_3)_2$···CO_2

Figure 3.11. The stable shapes of the complexes fromed between CH_3COCHR_2 and CO_2 (R= CH_3, F, Cl, Br)

Table 3.19. Interaction energies (kJ.mol^{-1}), BSSE (kJ.mol^{-1}),the changes in the bond length (Δr, mÅ), stretching frequency (Δν, cm^{-1}) of the C7–H8 bond in the complexes relative to the relevant monomers

	CH_3COCHR_2···CO_2						
	R1	R2(3)	ΔE	BSSE	ΔE*	Δr(C7H8)	Δν(C7H8)
R = H	2.87	2.61	-12.7	2.4	-10.4	-0.25	10.9
R = CH_3	2.85	2.77 2.79[b)]	-13.6	2.8	-10.7	-0.54 -0.54[a)]	14.1 6.0[a)]
R = F	2.94	2.51	-11.9	2.8	-9.2	-0.84	16.3
R = Cl	2.92	2.40	-13.8	3.8	-10.1	-0.68	15.0
R = Br	2.91	2.38	-13.8	2.4	-10.4	-0.65	14.8

[a)] For the C10–H17 bond in $CH_3COCH(CH_3)_2$···CO_2, [b)] For the value of R3

Table 3.20. Deprotonation enthalpy of the C–H bond of the –CHR_2 group and the proton affinity at the O site of the >C=O group in the relevant monomers (kJ.mol^{-1})

	CH_3COCH_3	$CH_3COCH(CH_3)_2$	CH_3COCHF_2	$CH_3COCHCl_2$	$CH_3COCHBr_2$
DPE	1704.6	1707.8	1669.9	1579.4	1558.4
PA	812.7	832.9	738.6	762.1	776.1

Obtained results show that the C–H···O hydrogen bonds in examined complexes belong to blue-shifting hydrogen bond. The magnitude of polarization of the C–H bond in the isolated monomers increases in going from F via Cl to Br. A decrease in the magnitude of the C-H bond length contraction and its stretching frequency enhancement in the complexes are observed (*cf.* Tables 3.19 and 3.20). This is not observed in the case of the CH_3 substitution group in the present work since the shape of the $CH_3COCH(CH_3)_2$···CO_2 complex differs from the remaining ones. Thus, the bond length contraction and the stretching frequency blue shift are inversely proportional to the polarization of the C-H bond in the initial monomers, and slightly dependent on the geometric structure of the complexes.

3.4.2. Interactions of XCN (X = F, Cl, Br) with CH_3COCHR_2 (R = H, CH_3, F, Cl, Br)

We now continue to investigate the interactions of CH_3COCHR_2 with XCN in order to evaluate the stability and the kind of C–H···N hydrogen bond. The stable complexes are similar to that of CH_3COCH_3···CO_2. There is only a slight difference in the structures when replacing the O12 and O13 atoms of CO_2 by the N12 and X13 atoms of XCN, respectively. Some of the typical data are tabulated in Table 3.22.

Table 3.22. Intermolecular contact distances (in Å), interaction energies (in kJ.mol^{-1}) and the changes in the bond length (in mÅ), stretching frequency (in cm^{-1}) of the C7–H8 bond in the complexes relative to the respective monomers

	CH_3COCHR_2···XCN					
	R1	R2(3)	ΔE	ΔE*	Δr(C7H8)	Δν(C7H8)
R = H, X = F	2.84	2.57	-16.7	-13.9	-0.13	10.0
R = H, X = Cl	3.09	2.55	-15.1	-11.8	-0.10	8.9
R = H, X = Br	3.13	2.56	-13.5	-11.1	-0.06	8.0
R = CH_3, X = F	2.82	2.76	-17.9	-14.4	-0.84	12.8
		2.74			-0.84[a)]	9.1[a)]
R = CH_3, X = Cl	3.06	2.74	-18.3	-12.4	-0.82	12.2
		2.76			-0.80[a)]	8.1[a)]
R = CH_3, X = Br	3.11	2.71	-15.1	-11.9	-0.81	12.0
		2.76			-0.80[a)]	8.1[a)]
R = F, X = F	2.89	2.46	-16.4	-13.0	-0.90	17.5
R = F, X = Cl	3.11	2.43	-16.0	-12.1	-0.78	15.8
R = F, X = Br	3.15	2.41	-14.8	-11.7	-0.76	15.4
R = Cl, X = F	2.87	2.33	-18.7	-14.1	0.09	-0.2
R = Cl, X = Cl	3.08	2.29	-18.5	-13.3	0.35	-0.4
R = Cl, X = Br	3.13	2.28	-17.4	-13.0	0.38	-0.8
R = Br, X = F	2.87	2.31	-18.6	-14.5	0.14	-1.2
R = Br, X = Cl	3.08	2.28	-18.4	-13.7	0.38	-1.8
R = Br, X = Br	3.13	2.27	-17.3	-13.4	0.40	-2.2

[a)] *For the C10–H17 bond*

The obtained results pointed out that the >C=O···C Lewis acid-base and C–H···N hydrogen bond interactions are formed in CH_3COCHR_2···XCN. Interaction energies of the complexes are significantly negative, and more negative than those of CH_3COCHR_2···CO_2, suggesting a larger stability of CH_3COCHR_2···XCN relative to CH_3COCHR_2···CO_2. As shown in Table 3.22, the strength of CH_3COCHR_2···FCN complexes increases in the order F < H < Cl < CH_3 ≈ Br, and H < F < CH_3 < Cl < Br for CH_3COCHR_2···ClCN and CH_3COCHR_2···BrCN. The stability of the complexes is contributed from both the >C=O···C Lewis acid-base interaction and the C–H···N hydrogen bond, since there are increases in both the C–H polarity and O-gas basicity on going from the F- via Cl- to Br-substituted derivative of CH_3COCHR_2. Thus, the C–H···N hydrogen bond is more stable than the C–H···O hydrogen bond.

The CH_3COCHR_2···XCN complexes are more stable than the complexes of CH_3COCHR_2···CO_2. This result is due to the values of PA at the N sites in XCN are larger than that at the O site in CO_2. Indeed, the value of PA at the O atom of CO_2 is 541.6 kJ.mol^{-1}, which is significantly smaller than the PAs at the N atoms of XCN (the PAs at

the N sites in FCN, ClCN and BrCN molecules calculated are 690.1, 733.9 and 747.5 kJ.mol^{-1}, respectively) (the value of PAs are at the CCSD(T)/6-311++G(3df,2pd)//MP2/6-311++G(2d,2p) level). These results firmly indicate a larger magnitude in the strength of the C–H···N interaction relative to the C–H···O interaction in stabilizing the complexes. In brief, substitution of the two H atoms in a CH_3 group of CH_3COCH_3 by two alike R groups (R = CH_3, F, Cl, Br) results in an increase in the strength of CH_3COCHR_2···XCN compared to CH_3COCH_3···XCN, while it negligibly affects the strength of CH_3COCHR_2···CO_2 relative to CH_3COCH_3···CO_2.

The results in Table 3.22 point out that the C7–H8···N12 hydrogen bond in the CH_3COCHR_2···XCN complexes belongs to the blue-shifting hydrogen bond in the case R = CH_3, H, F and the red shifting hydrogen bond in the case R = Cl, Br. In the case R = CH_3, H or F interacting with XCN, there is a tiny decrease in the magnitude of the shortening of the C7–H8 bond length and its stretching frequency increase on going from FCN to ClCN and then to BrCN. Going in the same this trend, an increase in the magnitude of the C7-H8 bond length elongation and its stretching frequency decrease is observed in each pair of CH_3COCHR_2···XCN (R = Cl, Br). These results are due to both an increase in the gas phase basicity at the N atoms from FCN to ClCN to BrCN, and a stronger polarization of the C7–H8 bonds in the CH_3COCHR_2 (R = Cl, Br) relative to the CH_3COCHR_2 (R = H, CH_3, F) molecules (*cf.* Table 3.20).

A red shift of the C7–H8 stretching frequency is predicted in CH_3COCHR_2···XCN complexes, with R = Cl and Br. In addition, as shown in Table 3.22, for each XCN, there is a shortened-to-lengthened change in the C7–H8 bond length and a blue-to-red shift of its stretching frequency in the examined complexes relative to the respective monomers. The obtained results should be firmly assigned to an increase in the polarity of the C7–H8 covalent bond on going from the CH_3 *via* H to F to Cl and finally to the Br substituted derivative. Thus, the blue shift of C–H bond involved in the C–H···N hydrogen bonds are inversely proportional to the polarization of the C bond and the gas phase basicity of the N atom in the initial monomers. The contraction of the C7–H8 bond length and the blue shift of its stretching frequency are larger for each of the CH_3COCHR_2···CO_2 series than for each of the CH_3COCHR_2···XCN series, respectively.

Summary

- The stability of the complexes is contributed by the crucial role of the >C=O···C Lewis acid-base interaction and an additional cooperation of the C–H···O/N hydrogen bonded interaction. Generally, the substitution of the two H atoms in a CH_3 group of CH_3COCH_3 by two alike R groups (R = H, CH_3, F, Cl, Br) leads to an increase in the strength of CH_3COCHR_2···XCN relative to CH_3COCH_3···XCN, while it negligibly affects the strength of CH_3COCHR_2···CO_2 relative to CH_3COCH_3···CO_2.

- The blue shift magnitude of C–H bond stretching frequency involved in the C–H···O/N hydrogen bonds are inversely proportional to the polarization of the C–H bond and the gas phase basicity of the O/N atom in the initial monomers, and slightly dependent on the geometrical complex.

3.7. Structure, stability and interactions in the complexes of carbonyls with cyanides

Interactions of RCHO (R = H, F, Cl, Br, CH_3 and NH_2) with XCN (X = H, F) induce twenty-two stable complexes in 3 different C_s-symmetry shapes which are symbolized

hereafter by **C1**, **C2** and **C3** corresponding to **C1(R-X), C2(R-X)** and **C3(R-X)** complexes as presented in Figure 3.17. Interaction energies of all the complexes at the CCSD(T)/aug-cc-pVTZ//MP2/aug-cc-pVDZ level are gathered in Table 3.32.

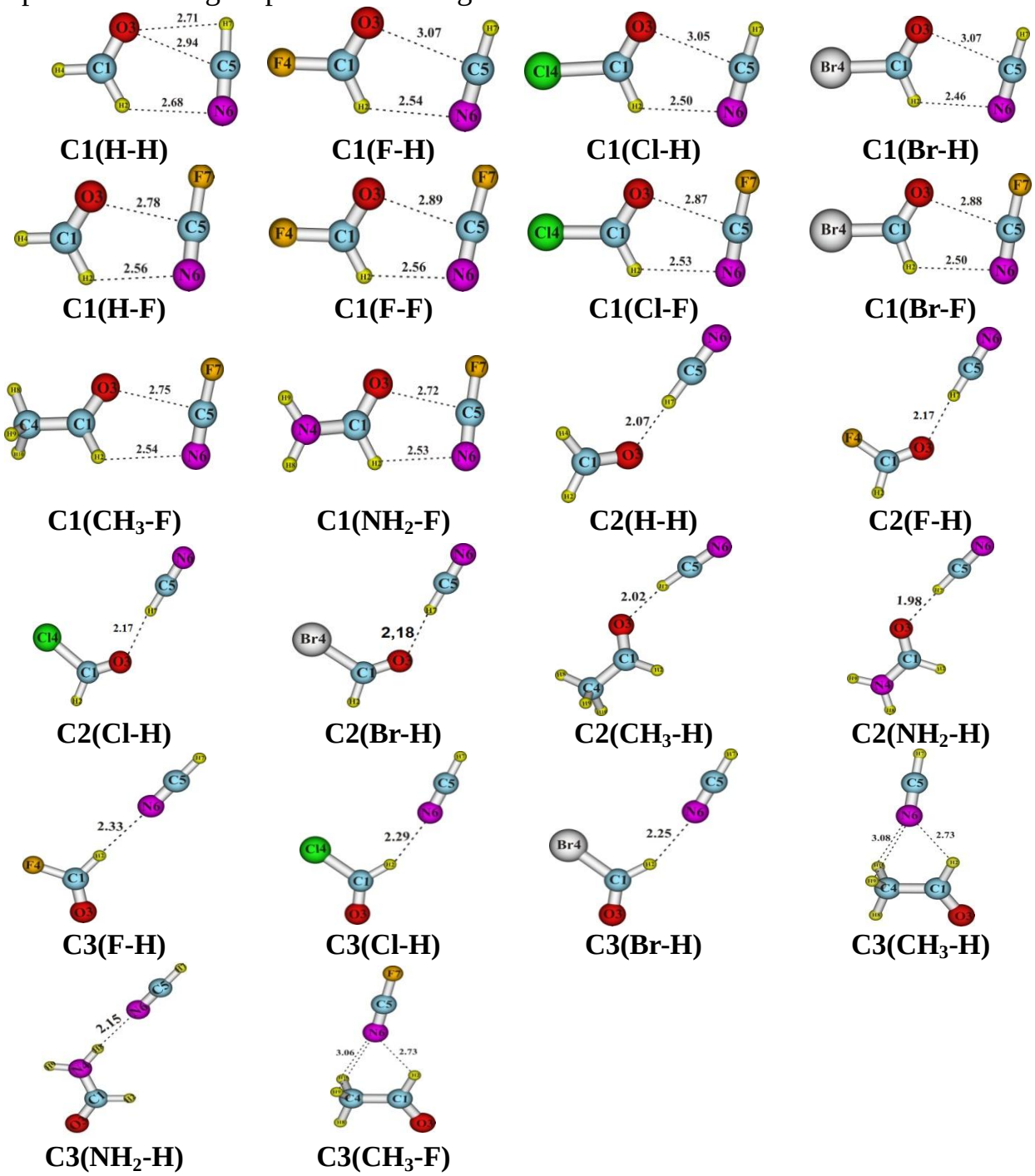

Figure. 3.17. Optimized geometrical structures of **C1(R-X)**, **C2(R-X)** and **C3(R-X)** complexes at the MP2/aug-cc-pVDZ level of theory

Intermolecular distances (Fig 3.17) point out the existence of C–H···N/O, N–H···N hydrogen bonds and C=O···C Lewis acid-base interactions in the examined complexes. The stability of the **C1(R-X)** complexes is contributed by both the >C=O···C Lewis acid-base interaction and the C–H···N hydrogen bond, while the **C2(R-X)** and **C3(R-X)** complexes are stabilized by the C–H···O, C–H···N and N–H···N hydrogen bonds. The **C1(CH_3-F)** and **C1(NH_2-F)** complexes should be more stable than the rest of **C1(R-F)** complexes (*cf.* Table 3.32). Interaction energies (ΔE^*) of the halogenated complexes in **C1**

shape are *ca* -12.0 kJ.mol^{-1} for RCHO···HCN and -13.0 kJ.mol^{-1} for RCHO···FCN, which are close to those of the non-substituted complexes, meaning that the substitution of one H atom in HCHO by one halogen atom in the **C1** shape negligibly affects the stability of the RCHO···XCN relative to HCHO···XCN complexes. To further understand the difference in stability of the **C1(R-X)** complexes upon substitution, the proton affinity at O site of the aldehydes and N site of the cyanides together with deprotonation enthalpy of C–H bond of the aldehydes at the CCSD(T)/aug-cc-pVDZ//MP2/aug-cc-pVDZ level are calculated, and the results are collected in Table 3.33.

Table 3.32. Interaction energies (in kJ mol^{-1}) of the complexes at the CCSD(T)/augcc-pVTZ//MP2/aug-cc-pVDZ level

	C1(H-H)	**C1(F-H)**	**C1(Cl-H)**	**C1(Br-H)**	**C1(H-F)**	**C1(F-F)**
ΔE^*	-12.5	-12.1	-12.0	-12.0	-12.5	-12.8
	C1(Cl-F)	**C1(Br-F)**	**C1(CH_3-F)**	**C1(NH_2-F)**	**C2(H-H)**	**C2(F-H)**
ΔE^*	-12.7	-12.6	-14.6	-17.4	-14.2	-10.7
	C2(Cl-H)	**C2(Br-H)**	**C2(CH_3-H)**	**C2(NH_2-H)**	**C3(F-H)**	**C3(Cl-H)**
ΔE^*	-10.5	-10.2	-17.9	-22.6	-10.9	-10.9
	C3(Br-H)	**C3(CH_3-H)**	**C3(NH_2-H)**	**C3(CH_3-F)**		
ΔE^*	-11.4	-6.7	-14.8	-6.2		

Table 3.33. Deprotonation enthalpies and proton affinities (all in kJ.mol^{-1}) in RCHO, XCN monomers at the CCSD(T)/aug-pVDZ//MP2/aug-cc-pVDZ level

Monomer	HCHO	FCHO	ClCHO	BrCHO
DPE(C–H)	1681.9	1579.7	1530.4	1497.2
PA(O/N)	709.5	649.0	685.2	694.3
Monomer	CH_3CHO	NH_2CHO	HCN	FCN
DPE(C–H)	1654.3	1636.7/1533.0[a)]	1460.0	-
PA(O/N)	767.7	831.3	704.5[b)]	677.5[b)]

[a)]*for N–H bond and* [b)]*for N atom*

As shown in Table 3.33, the polarity of the C-H bond in RCHO decreases in the order Br > Cl > F > NH_2 > CH_3 > H, implying a decreasing strength of the C–H···N hydrogen bond in this order. On the other hand, the gas phase basicity at the O site of RCHO decreases in the order NH_2 > CH_3 > H > Br > Cl > F. Consequently, the larger strength of **C1(NH_2-F)** and **C1(CH_3-F)** relative to the remaining **C1(R-X)** complexes is accounted for a larger contribution of the >C=O···C Lewis acid-base interaction as compared to the contribution of the C–H···N hydrogen bond to overall stabilization energy. The decreasing stability of complexes occurs in the order of NH_2 > CH_3 > H > Br ≈ Cl ≈ F substituted derivative, which is consistent with the decreasing direction of proton affinity at the O site of RCHO. The predominating strength of **C2(H-H), C2(CH_3-H) and C2(NH_2-H)** as compared to the rest of complexes examined indicated a stronger interaction of the C_{sp}–H···O relative to C_{sp2}–H···N hydrogen bond.

The stability of the **C3(R-X)** complexes is contributed by the C–H···N and/or N–H···N hydrogen bonds. Complex strength decreases in going from NH_2 > Br > Cl > F > CH_3 derivatives. This trend is consistent with an increasing in polarity of C–H or N–H covalent bond in the order of CH_3 < F < Cl < Br < NH_2 substituted derivatives (*cf.* Table 3.32 and Table 3.33). In the **C3** shape, the **C3(NH_2-H)** complex is the most stable and the **C3(CH_3-**

F) is the least stable. The largest strength of **C3(NH_2-H)** is caused by the strongest polarization of the N–H bond in NH_2CHO as compared to C_{sp2}–H (–CHO) bond. The least stable **C3(CH_3-F)** complex should be accounted for the C–H···N weak hydrogen bonds owing to the weaker gas phase basicity at the N site of FCN compared to HCN.

The changes of bond length, stretching vibration frequency of C/N–H bonds involved the C–H···N/O and N–H···N hydrogen bonds are gathered in Table 3.34.

Table 3.34. Changes in bond length and stretching vibrational frequency of the C/N–H bond involved in hydrogen bonds of the complexes

Complexes	Δr(C/N–H)	Δν(C/N–H)	Complexes	Δr(C/N–H)	Δν(C/N–H)
C1(H-H)	-0.0015	23.0	**C2(Cl-H)**	0.0040	-59.2
	-0.0005[a)]	5.9[a)]	**C2(Br-H)**	0.0038	-56.7
C1(F-H)	-0.0002	6.2	**C2(CH_3-H)**	0.0101	-151.0
C1(Cl-H)	-0.0005	10.1	**C2(NH_2-H)**	0.0117	-173.0
C1(Br-H)	-0.0005	9.6	**C3(F-H)**	-0.0004	15.2
C1(H-F)	-0.0008	12.6	**C3(Cl-H)**	-0.0014	31.5
C1(F-F)	-0.0007	13.1	**C3(Br-H)**	-0.0013	30.6
C1(Cl-F)	-0.0004	8.4	**C3(CH_3-H)**	-0.0034	41.9
C1(Br-F)	-0.0019	29.3	**C3(NH_2-H)**	-0.0007 [b)]	3.7 [b)]
C1(CH_3-F)	-0.0030	40.7		0.0046[c)]	-36.9[c)]
C1(NH_2-F)	-0.0021	29.3	**C3(CH_3-F)**	-0.0032	39.0
C2(H-H)	0.0073	-107.8		-0.0007[b)]	3.7[b)]
C2(F-H)	0.0038	-56.7			

[a] *For C5–H7 bond in **P1(H-H)**,* [b] *for C4–H9(10) bonds in **P3(CH_3-H(F))** and* [c] *for N4–H8 in **P3(NH_2-H)***

The results show that, all the C_{sp}–H···O, C_{sp2}–H···N and C_{sp3}–H···N interactions in the **C1(R-X)** and **C3(R-X)** complexes are blue-shifting hydrogen bonds. The larger contraction and stretching frequency increase of C_{sp2}–H covalent bonds are found in **C1(CH_3-F)** and **C1(NH_2-F)** relative to the rest **C1(R-X)** complexes, and they generally approximate to each other in the halogenated complexes of **C1** shape (accept **C1(Br-F)**). This proposes that the substitution of one H atom in HCHO by an electron-donating group such as CH_3, NH_2 increases the blue shift of the C_{sp2}–H bond in the C_{sp2}–H···N hydrogen bond, while it makes the negligible change of the C_{sp2}–H blue shift in the case of the halogenated complexes of **C1** shape, as compared to that in **C1(H-H)** and **C1(H-F)**. The blue shift of C_{sp2}–H bond involved in the C_{sp2}–H···N hydrogen bond is larger for **C1(R-F)** than for **C1(R-H),** which is due to the stronger gas phase basicity at the N site of HCN compared to FCN.

In the **C2(R-H)** and **C3(NH_2-H)** complexes, the C_{sp}–H···O and N–H···N hydrogen bonds are red-shifting hydrogen bonds. The larger red shift of C_{sp}–H bond involving the C_{sp}–H···O hydrogen bond in the **C2(R-H)** complexes relative to that of N–H bond involving N–H···N hydrogen bond in **C3(NH_2-H)** is observed. This result should be assigned to the larger polarity of C_{sp}–H bond in HCN compared to N–H bond in NH_2CHO. The red shift of C_{sp}–H bond involving in the C_{sp}–H···O hydrogen bond in the **P2** complexes increases in the order of F ≈ Cl ≈ Br < H < CH_3 < NH_2 substituted group, which is due to the enhanced gas-phase basicity at O site of RCHO in this order. In summary, the type of hydrogen bond and the magnitude of changes in the C–H bond

length and its stretching frequency is inversely proportional to the polarization of the donor proton and the gas phase basicity of the accepted proton in the initial monomers.

To elucidate the role of various factors contributing to overall stabilization of complexes, interaction energies are decomposed into different terms related to physically well-defined components using SAPT2+ approach with aug-cc-pVDZ basis set, the results are selected in Table 3.35.

Table 3.35. Components in the interaction energy (kJ mol^{-1}), with the aug-cc-pVDZ basis set

Complexes	E_{elest}	E_{ind}	E_{disp}	E_{exch}	δE^{HF}	E^{SAPT}
C1(H-H)	-21.7(50)	-8.6(20)	-10.5(24)	26.7	-2.3(5)	-16.4
C1(F-H)	-18.7(51)	-7.1(19)	-9.1(25)	22.6	-1.7(5)	-14.0
C1(Cl-H)	-18.8(48)	-7.8(20)	-10.2(26)	25.2	-2.1(5)	-13.7
C1(Br-H)	-186(48)	-7.8(20)	-10.4(27)	25.6	-2.2(6)	-13.4
C1(H-F)	-27.0(46)	-15.4(26)	-13.8(23)	40.6	-2.7(5)	-18.3
C1(F-F)	-22.4(48)	-11.2(24)	-11.5(25)	31.4	-1.8(4)	-15.4
C1(Cl-F)	-22.3(46)	-11.8(24)	-12.6(26)	33.6	-2.1(4)	-15.2
C1(Br-F)	-22.2(45)	-11.9(24)	-12.9(26)	34.4	-2.2(5)	-14.8
C1(CH_3-F)	-29.4(45)	-17.6(27)	-15.1(23)	45.1	-3.0(5)	-20.1
C1(NH_2-F)	-34.5(46)	-21.0(28)	-16.1(21)	51.3	-3.3(4)	-23.7
C2(H-H)	-27.1(56)	-9.7(20)	-8.1(17)	26.2	-3.5(5)	-22.1
C2(F-H)	-17.9(55)	-6.0(19)	-6.3 (20)	16.7	-2.0(6)	-15.5
C2(Cl-H)	-17.6(51)	-7.0(20)	-7.6(22)	18.6	-2.3(7)	-15.8
C2(Br-H)	-16.7(48)	-7.4(21)	-8.3(24)	19.5	-2.3(7)	-15.2
C2(CH_3-H)	-32.7(55)	-12.7(21)	-9.7(16)	33.5	-4.7(8)	-26.4
C2(NH_2-H)	-39.3(56)	-14.5(21)	-10.5(15)	38.1	-5.6(8)	-31.9
C3(F-H)	-18.9(61)	-4.6(15)	-6.0(19)	15.4	-1.6(5)	-15.7
C3(Cl-H)	-18.9(58)	-5.1(16)	-6.7(21)	16.5	-1.8(5)	-15.9
C3(Br-H)	-20.5(55)	-6.4(17)	-8.5(23)	20.4	-2.2(6)	-17.1
C3(CH_3-H)	-9.5(51)	-2.5(13)	-6.3(34)	8.7	-0.5(3)	-10.0
C3(NH_2-H)	-26.0(58)	-7.9(18)	-8.4(19)	23.6	-2.5(6)	-21.1
C3(CH_3-F)	-8.8(48)	-2.4(13)	-6.5(36)	8.9	-0.5(3)	-9.2

Values in brackets are the contribution percentage of the energy component in the total interaction energy of the complex

For all the twenty-two complexes, electrostatic component plays the most important role in the strength of Lewis acid-base and hydrogen-bonded interactions, which is about 50% in stabilization energy of the complexes. Generally, the induction and dispersion terms play a similar role and are about half of the attractive energy term to the overall interaction energy. They thus range from 13 to 28% for the former and from 15 to 36% for the latter. Accordingly, the strength of examined complexes significantly depends on the contribution of three energy components: electrostatic, induction and dispersion terms, while the first overcomes the latter. The δE^{HF} component contributes to the stability of complexes with less extent, only from 3 to 8%. The electrostatic term is enhanced up to 5%, while the induction and dispersion terms are decreased by about 5% in the **C2(R-H)** complexes possessing the red-shifting hydrogen bond as compared to the rest of the complexes.

We performed AIM analysis at the MP2/aug-cc-pVDZ level for all of complexes, and evaluated the relationship between the interaction energy (ΔE^*), kinetic (G(r)) and potential (V(r)) energy densities at BCPs with the intermolecular distances (R(H)) of the hydrogen bonds in the **C2(R-X)** and **C3(R-X)** complexes (except for **C3(CH_3-H)** and **C3(CH_3-F)**), which are found as following expressions:

$\Delta E^* = -2.63x10^3 exp(-2.4607R(H))$ (1)

$V(r) = -5.61x10^3 exp(-2.4607R(H))$ (2)

$G(r) = 6.16x10^3 exp(-2.4607R(H))$ (3)

Consequently, the relationship of the energy terms is obtained by the expressions: $\Delta E^* \approx 0.47$ V(r) (*) and $\Delta E^* \approx -0.43$ G(r) (**). We use the both of expressions to calculate the interaction energy of each interaction in the ring complexes. The calculated results according to the (*) and (**) expressions are gathered in Table 3.37.

Table 3.37. Interaction energies of the intermolecular contacts in the ring complexes calculated (*) and (**) expressions

Complexes	$\Delta E^* \approx 0,47V(r)$ (*)		$\Delta E^* \approx -0,43G(r)$ (**)	
	ΔE(Lewis) of (C1=O3···C5)	ΔE(H) of (C1-H2···N6)	ΔE(Lewis) of (C1=O3···C5)	ΔE(H) of (C1-H2···N6)
C1(H-H)	-7.1	-7.1[a)] -4.6	-8.5	-7.8[a)] -5.6
C1(F-H)	-4.8	-5.6	-6.0	-6.6
C1(Cl-H)	-5.0	-6.3	-6.2	-7.2
C1(Br-H)	-4.9	-6.9	-6.0	-7.8
C1(H-F)	-10.3	-7.8	-11.1	-7.4
C1(F-F)	-7.8	-8.6	-8.8	-8.1
C1(Cl-F)	-8.7	-7.1	-9.2	-6.9
C1(Br-F)	-7.5	-6.6	-8.8	-7.7
C1(CH_3-F)	-11.6	-7.4	-12.4	-7.6
C1(NH_2-F)	-11.5	-6.3	-12.6	-7.4

[a)] *for C5–H7···O3 hydrogen bond*

The obtained interaction energies for each intermolecular contact are close to each other for both the (*) and (**) expressions. It is remarkable that the stability of the RCHO···FCN complexes in **C1** shape is mainly contributed by the C1=O3···C5 Lewis acid-base interaction, while that of the RCHO···HCN complexes in **C1** shape is determined by the C1–H2···N6 hydrogen bond. Individual energies of C_{sp3}–H···N is very small, in the range of 3 to 4 kJ.mol^{-1}, which is smaller than that of C_{sp2}–H···N (*ca.* 4-9 kJ.mol^{-1}) and N–H···N (*ca.* 14 kJ.mol^{-1}). Individual energies of the C_{sp}–H···O hydrogen bonds are largest with the values of 11-21 kJ.mol^{-1}.

Summary

- It is found that the larger stability and red shifting of its stretching frequency of C_{sp}–H···O hydrogen bonds relative to that of N–H···N hydrogen bonds and *via* C_{sp2}–H···N hydrogen bonds.

- AIM analysis show that the expressions of correlation between the interaction energy and the kinetic and potential energy densities in the: $\Delta E^* \approx 0.47$ V(r) and $\Delta E^* \approx -0.43$ G(r). Individual energies of C_{sp3}–H···N is very small, in the range of 3 to 4

kJ.mol^{-1}, which is smaller than that of C_{sp2}–H···N (*ca.* 4-9 kJ.mol^{-1}) and N–H···N (*ca.* 14 kJ.mol^{-1}). Individual energies of the C_{sp}–H···O hydrogen bonds are largest with the values of 11-21 kJ.mol^{-1}.

- The SAPT2+ analysis shows the attractive electrostatic term overcoming both the induction and dispersion terms in stabilizing all the RCHO···XCN complexes.

- The blue shifting magnitude of stretching frequency of the C/N–H involved in the hydrogen bonds are inversely proportional to the polarization of C/N–H bonds and the gas phase basicity of the proton acceptors in the initial monomers

3.8. A theoretical study of structure, stability and hydrogen bond in the complexes formed between cytosine and guanine

The cytosine-guanine complexes were selected to investigate for purpose of further understanding the formation and stability of the C/N–H···O/N hydrogen bonds. The stable geometric structure, and intermolecular distances for the complexes at the B3LYP/6-311++G(2d,2p) level are shown in Figure 3.20.

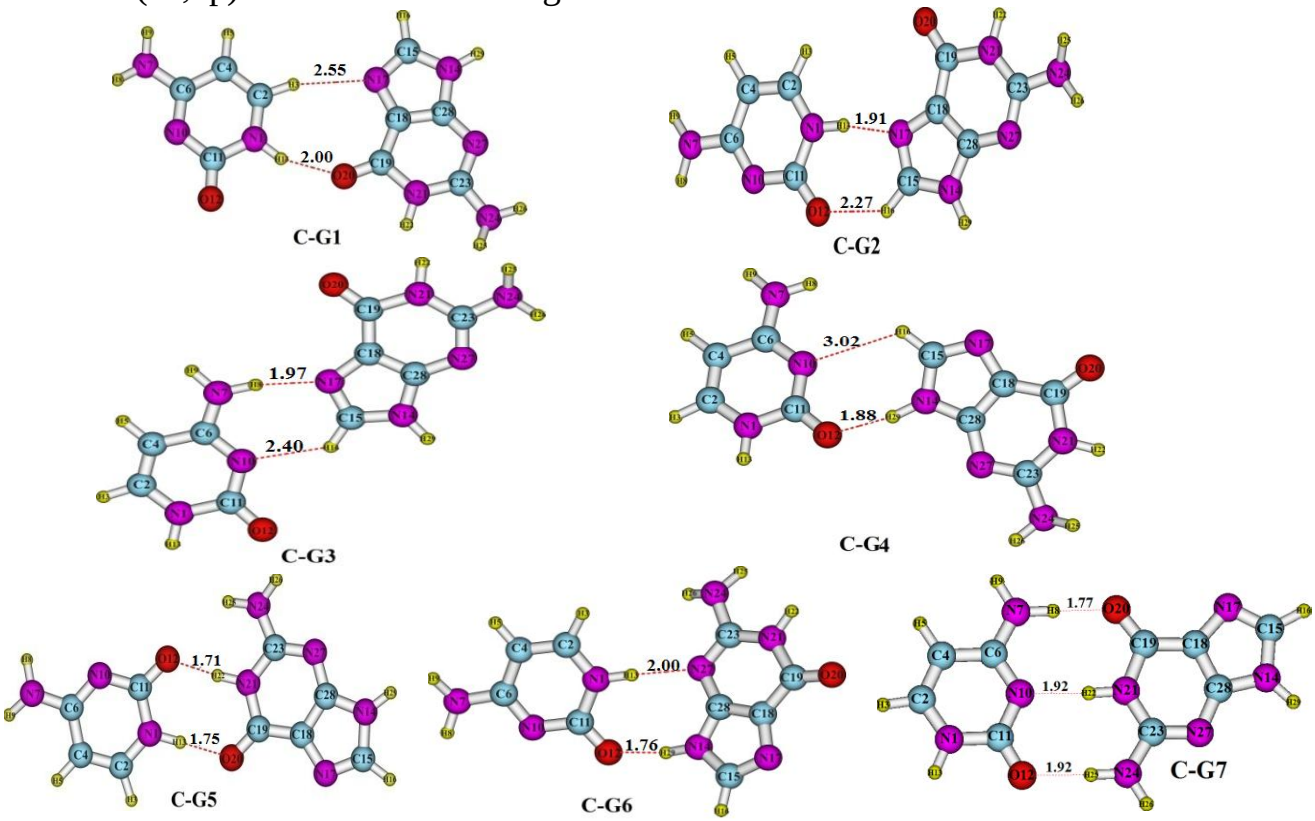

Figure 3.20. The stable structures of the cytosine-guanine complexes

The interaction energies of the complexes are quite negative, ranging from -7.4 to -20.3 kcal.mol^{-1} for ZPE and ZPE+BSSE corrections respectively, implying the obtained complexes are quite stable. The DPE values of N24–H25, N1–H13, N7–H8, N14–H29 bonds are 338.8, 356.2, 354.1 and 337.1 kcal.mol^{-1}, respectively, where as the DPE values of the C2–H3 and C15–H16 bonds are in turn 370.2 and 379.1 kcal.mol^{-1}. For the PA values at the O/N atom, they decrease in the order of N17 (229.9) > N10 (228.6) > O12 (221.4) > O20 (216.4) > N27 (312.1) (all in kcal.mol^{-1}). These results indicate that the N–H···O/N hydrogen bonds play a more important than C–H···O/N hydrogen bonds into total stabilization energy.

The results from Table 3.41 point to that the C/N–H···O/N hydrogen bonds in the complexes are red-shifting hydrogen bonds. Notably, the red shift of N–H bond in the N–

H···O/N hydrogen bonds is much larger than that of C–H in the C–H···O/N hydrogen bonds, which is in good agreement with the larger polarity of N–H bond compared to the C–H bond. In contrast, the C15–H16···N10 hydrogen bond exhibits the blue shift in the complex **C-G4**. Intermolecular hyperconjugative energies of electron density transfer from n(O/N) to σ*(C/N–H) involved in N–H···O/N hydrogen bonds are larger than that of hydrogen bond of the C–H···O/N, affirming that N–H···O/N hydrogen bonds play more decisive role than the C–H···O/N hydrogen bonds in stabilizing the complexes of cytosine and guanine. AIM analysis also shows that the energies of the N–H···O/N hydrogen bonds are in the range of 4.7-13.3 kcal.mol^{-1}, that are much larger than the C–H···O/N hydrogen bonds (*ca.* 0.6-2.7 kcal.mol^{-1}). The SAPT analysis indicate that the total stabilization energy of the complex is mainly contributed by the electrostatic component (45-55%), the rest by the induction energy (21-32%), the dispersion (12 -17%), induction and induction-exchange (5-10%).

Table 3.41. Changes in bond length (Δr), stretching frequency (Δν) of C–H, N–H bonds, and NBO analysis

Complexes	Hydrogen bond	Δr(C/N-H) (Å)	Δν(C/N-H) (cm^{-1})	EDT (e)	E_{inter} [a)] (kcal.mol^{-1})
C-G1	C2–H3···N17	0.002	-13.5	-0.020	2.0
	N1–H13···O20	0.007	-106.6		6.5
C-G2	N1–H13···N17	0.020	-369.8	-0.030	16.7
	C15–H16···O12	0.002	-17.3		2.6
C-G3	N7–H8···N17	0.017	-318.6	-0.020	13.2
	C15–H16···N10	0.002	-18.7		2.5
C-G4	C15–H16···N10	-0.001	10.7	0.035	0.4
	N14–H29···O12	0.016	-284.3		13.9
C-G5	N21–H22···O12	0.028	-544.7	0.007	29.6
	N1–H13···O20	0.029	-505.0		24.4
C-G6	N1–H13···N27	0.017	-319.7	0.010	13.1
	N14–H29···O12	0.025	-441.0		21.7
C-G7	N24–H25···O12	0,0107	-232,4	0,018	12,8
	N21–H22···N10	0,0195	-371,7		20,0
	N7–H8···O20	0,0265	-506,8		24,8

[a)] *intermolecular hyperconjugative energy from n(O/N) to σ*(C/N–H)*

Summary

- The obtained complexes are quite stable with interaction energies in the range from -7.4 to -22.7 kcal.mol^{-1} with both ZPE and BSSE corrections. The strength of the complexes is mainly contributed by the N–H···O/N hydrogen bonds overcoming the role of the C–H···O/N hydrogen bonds.

- The hydrogen bonds examined belong to the red-shifting hydrogen bond, in which the larger red shift is observed for N–H···O/N hydrogen bonds than for the C–H···O/N hydrogen bonds. This is due to the stronger polarization of the N–H bond in the initial monomer in comparison with the C–H bond, except for the weak C–H···N blue-shifting hydrogen bond found in the complex C-**G4**.

CONCLUSION

From the study of 8 complex systems including 134 structures at selected levels of theory, we have obtained some remarkable conclusions as follows:

1) The C–H···O/N blue-shifting hydrogen bonds and the O–H···O/N, N–H···O/N and C–H···O/N red-shifting hydrogen bonds are found in the systems investigated. Their presence and stability are also investigated and evaluated in the complexes of cytosine and guanine. Moreover, other noncovalent interactions such as chalcogen-chalcogen, π···π*, p···π* and Lewis acid-base interactions are also observed in some complexes. Remarkably, the contribution of the π···π* interaction to the complex formed between CO_2-philic compounds and CO_2 has been revealed for the first time in interaction of ethylene with CO_2. The presence of the C–H···O blue-shifting hydrogen bonds in complexes of methanol and ethanol with CO_2 has also not been reported previously.

2) The contracted magnitude of the C–H bond length and the increase of its stretching frequency involved in the C–H···O/N hydrogen bonds are inversely proportional to the polarization of the C–H bond and the gas phase basicity of the O/N atom in the isolated monomers, and slightly dependent on the geometric structure of the complex. The O–H···O/N, N–H···N/O and C–H···O/N red-shifting hydrogen bonds are the result from electrostatic force, and their red shift is directly proportional to the polarity of the O/N/C–H bonds and gas phase basicity of the O/N atoms in proton donor and proton acceptor, respectively.

3) The C–H···O/N hydrogen bonds are weak hydrogen bonds with the individual energy to be from 3 to 11 $kJ.mol^{-1}$, and the the N–H···O/N ones belong to medium hydrogen bond with the binding energies ranging from 14 to 50 $kJ.mol^{-1}$. Remarkably, the C_{sp}–H···O hydrogen bond exhibits the red shift with its binding energy up to 21 $kJ.mol^{-1}$, belonging to medium hydrogen bond type, is found in the complexes of carbonyls and cyanides. As a result, the N–H···O/N bond hydrogens are more stable than the C–H···O/N ones.

4) For the monomers of C_2H_3X, XCH=CHX, XCH_2OH, CH_3SZCHR_2, CH_3COCHR_2, XNHCHO, RCHO, XCN, when X is replaced by halogens (F, Cl, Br), the strength of the obtained complexes is almost unchanged, however, it is increased when X is replaced by CH_3 and NH_2 groups as compared to the corresponding complexes of X to be H atom.X=H

5) The obtained results from SAPT2+ analysis indicate that the total stabilization energy of the complexes is contributed by three energy components: electrostatic, induction and dispersion terms, in which the first one overcoming two latter ones plays a main role in stabilizing complexes, and two latter ones occupies an close role.

6) The presence of the Lewis acid-base interactions >C=O···C, C–X···C, O=C···O and >S=Z···C (Z = O, S) in the complexes is resulted from the electron density transfer from the n(O/S/X) orbital to π*(C=O/N) orbital. The formation of the chalcogen-chalcogen interactions is caused by the transfer of electron density from n(O) to π*(Z = S) orbital. Especially, the electron density transfer from n(O) to π*(C=O) orbital and from π(C=C) to π(C=O) orbital, and vice versa are responsible for the existence of p···π* and π···π* interactions, respectively.

LIST OF THE PUBLICATIONS

1. Đỗ Thanh Hiền, Nguyễn Thị Thu Trang, Nguyễn Tiến Trung, Trần Thành Huế (2012), "Sự chuyển dời xanh của liên kết C-H và N-H trong các phức giữa đimetyl ete và dẫn xuất thế halogen của nó với HNO", *Tạp chí Hóa học*, 50(3), 295-300.
2. Trần Thị Phương Oanh, Võ Thúy Phượng, Nguyễn Ngọc Trí, Nguyễn Thị Thu Trang, Nguyễn Tiến Trung (2013), "Nghiên cứu lý thuyết tương tác của XCH_2OH (X = H, CH_3, F, Cl, Br) với CO_2", *Tạp chí Hóa học*, 51(3), 327-331.
3. Vo Thuy Phuong, Nguyen Thi Thu Trang, Vien Vo, Nguyen Tien Trung (2014), "A comparative study on interaction capacity of CO_2 with the >S=O and >S=S groups in some doubly methylated and halogenated derivatives of CH_3SOCH_3 and CH_3SSCH_3", *Chemical Physics Letters*, 598, 75-80.
4. Ho Quoc Dai, Nguyen Ngoc Tri, Nguyen Thi Thu Trang, Nguyen Tien Trung (2014), "Remarkable effects of substitution on stability of complexes and origin of the C-H···O(N) hydrogen bonds formed between acetone's derivative and CO_2, XCN (X = F, Cl, Br)", *RSC Advances*, 4, 13901-13908.
5. Phạm Ngọc Khánh, Ngô Thị Thanh Phương, Nguyễn Lê Tuấn, Phạm Vũ Nhật, Trần Thành Huế, Nguyễn Thị Thu Trang, Nguyễn Tiến Trung (2015), "Nghiên cứu vai trò của các tương tác trong việc làm bền các phức giữa CO_2 với C_2H_3X (X = H, F, Cl, Br)", *Tạp chí Hóa học*, 53(1), 17-22.
6. Nguyễn Thị Thu Trang, Nguyễn Ngọc Trí, Nguyễn Mai Phượng, Nguyễn Tiến Trung (2015), "Ảnh hưởng của nhóm thế đến liên kết hydro chuyển dời xanh trong các phức của sự tương tác giữa RCHO với CH_3CHO (R = H, F, Cl, Br, CH_3, NH_2)", *Tạp chí Hóa học*, 53(4), 409-413.
7. Nguyễn Thị Thu Trang, Trần Thành Huế, Nguyễn Tiến Trung (2015), "Nghiên cứu liên kết hydro và độ bền của phức tương tác giữa NH_2CHO và XNHCHO (X = F, Cl, Br, CH_3) với H_2O bằng phương pháp hóa học lượng tử", *Tạp chí Khoa học và Công nghệ*, 53(1B), 413-422.
8. Vũ Hữu Tú, Nguyễn Thị Thu Trang, Nguyễn Tiến Trung (2016), "Nghiên cứu lý thuyết tương tác giữa cytosine và guanine: cấu trúc, độ bền và liên kết hydro", *Tạp chí Hóa học*, 54(5e1,2), 160-165.
9. Nguyen Tien Trung, Nguyen Thi Thu Trang, Vu Thi Ngan, Duong Tuan Quang, Minh Tho Nguyen (2016), "Complexes of carbon dioxide with dihalogenated ethylenes: structure, stability and interaction", *RSC Advances*, 6, 31401-31409.
10. Nguyen Ngoc Tri, Nguyen Thi Hong Man, Nguyen Le Tuan, Nguyen Thi Thu Trang, Duong Tuan Quang, Nguyen Tien Trung (2017), "Structure, stability and interactions in the complexes of cacbonyls with cyanides", *Theorytical Chemistry Accounts, 136:10*.